PHYSICAL REVIEW E **91**, 012140 (2015)

Second law and entropy production in a nonextensive system

Mauricio S. Ribeiro,* Gabriela A. Casas,† and Fernando D. Nobre‡
Centro Brasileiro de Pesquisas Físicas and National Institute of Science and Technology for Complex Systems, Rua Xavier Sigaud 150, 22290-180 Rio de Janeiro-RJ, Brazil
(Received 27 November 2014; published 26 January 2015)

A model of superconducting vortices under overdamped motion is currently used for describing type-II superconductors. Recently, this model has been identified to a nonlinear Fokker-Planck equation and associated to an entropic form characteristic of nonextensive statistical mechanics, $S_2(t) \equiv S_{q=2}(t)$. In the present work, we consider a system of superconducting vortices under overdamped motion, following an irreversible process, so that by using the corresponding nonlinear Fokker-Planck equation, the entropy time rate $[dS_2(t)/dt]$ is investigated. Both entropy production and entropy flux from the system to its surroundings are analyzed. Molecular dynamics simulations are carried for this process, showing a good agreement between the numerical and analytical results. It is shown that the second law holds within the present framework, and we exhibit the increase of $S_2(t)$ with time, up to its stationary-state value.

DOI: 10.1103/PhysRevE.91.012140 PACS number(s): 05.70.Ln, 05.40.Fb, 05.20.−y, 05.40.Jc

I. INTRODUCTION

The statistical definition of entropy in terms of probabilities allows a direct connection between the microscopic (described by statistical mechanics) and macroscopic (described by thermodynamics) worlds. One of the most relevant results that follows from this definition is the H theorem, which may be proved in several ways, e.g., by making use of a master equation or a Fokker-Planck equation. In the latter case, the H theorem is well established by considering the Boltzmann-Gibbs (BG) entropy and employing the linear Fokker-Planck equation [1,2]; therefore, one associates BG entropy with the linear Fokker-Planck equation and, consequently, with the wide range of physical phenomena described by this equation.

Recently, the proof of the H theorem has been generalized to take into account entropic forms different from the BG case [3–10]. In this way, the H theorem was achieved by associating generalized entropic forms with nonlinear Fokker-Planck equations (NLFPEs). Since NLFPEs are accepted nowadays to be related with many complex phenomena, such as those exhibiting anomalous diffusion [11], this general proof guarantees that such complex systems should be described by entropic forms more general than the BG entropy. For this, one may consider a NLFPE written in a very general form [3,7,8],

$$\eta \frac{\partial P(x,t)}{\partial t} = -\frac{\partial\{A(x)\Psi[P(x,t)]\}}{\partial x} + D\frac{\partial}{\partial x}\left\{\Omega[P(x,t)]\frac{\partial P(x,t)}{\partial x}\right\}, \quad (1)$$

where η represents an effective friction coefficient, D is a constant with dimensions of energy, and the external force $A(x)$ is associated with a potential $\phi(x)$ $[A(x) = -d\phi(x)/dx]$. The functionals $\Psi[P(x,t)]$ and $\Omega[P(x,t)]$ should satisfy certain mathematical requirements, e.g., positiveness [7,8], and one notices that the linear Fokker-Planck equation is recovered from Eq. (1) by choosing these functionals as $\Psi[P(x,t)] = P(x,t)$ and $\Omega[P(x,t)] = 1$. Furthermore, to ensure normalizability of $P(x,t)$ for all times, one must impose the conditions

$$P(x,t)|_{x\to\pm\infty} = 0, \quad \left.\frac{\partial P(x,t)}{\partial x}\right|_{x\to\pm\infty} = 0,$$
$$A(x)\Psi[P(x,t)]|_{x\to\pm\infty} = 0 \ \ (\forall t). \quad (2)$$

Due to the presence of an external potential $\phi(x)$, the H theorem corresponds to a well-defined sign for the time derivative of the free-energy functional,

$$F = U - \theta S, \quad U = \int_{-\infty}^{\infty} dx\, \phi(x)P(x,t), \quad (3)$$

with θ representing a positive parameter with dimensions of temperature. Moreover, the entropy is considered in the form

$$S[P] = k\int_{-\infty}^{\infty} dx\, g[P(x,t)], \quad g(0) = g(1) = 0, \ \frac{d^2g}{dP^2} \leqslant 0, \quad (4)$$

where k denotes a positive constant with dimensions of entropy, and the functional $g[P(x,t)]$ should be at least twice differentiable. Considering the NLFPE of Eq. (1), as well as a negative sign for the time derivative of the free energy [7–10], one gets that the functionals of Eq. (1) should be directly related to the entropic form,

$$-\frac{d^2g[P]}{dP^2} = \frac{\Omega[P]}{\Psi[P]}, \quad (5)$$

and we are assuming that $D = k\theta$.

The second law of thermodynamics, which is directly related to the H theorem, states that the entropy of an isolated system always increases for irreversible processes; this leads to the interesting phenomenon of entropy production [1,12–14]. Within the statistical definition of entropy, the entropy production yields a direct dependence on the time derivative of the corresponding probability; for this purpose, one may use, e.g., the Boltzmann, or Fokker-Planck equations in the case of continuous probabilities [1], or the master equation, when dealing with discrete probabilities [15]. Most investigations in the literature are concerned with the production of BG entropy

*ribeiro@cbpf.br
†Corresponding author: gabrielaa@cbpf.br
‡fdnobre@cbpf.br

(see, e.g., Refs. [1,15–17]), and so one makes use either of the standard master equation or the linear Fokker-Planck equation.

Within the framework of generalized entropies, the phenomenon of entropy production has been rarely studied in the previous literature (see, e.g., Refs. [18–22] for exceptions). Recently, the formalism was extended to general entropic forms for continuous probabilities [making use of the NLFPE in Eq. (1)] [21], as well as for discrete probabilities (using a generalized master equation) [22]. In the former case, it became convenient to express Eq. (1) as a continuity equation,

$$\frac{\partial P(x,t)}{\partial t} = -\frac{\partial J(x,t)}{\partial x},$$
$$J(x,t) = \frac{1}{\eta}\left\{A(x)\Psi[P] - D\Omega[P]\left[\frac{\partial P(x,t)}{\partial x}\right]\right\}. \quad (6)$$

Then, one may write the entropy time rate in the form [1,12–14]

$$\frac{d}{dt}S[P] = \Pi - \Phi, \quad (7)$$

where one identifies the entropy production Π and entropy flux Φ contributions. These two concepts were extended for the general entropic form defined in Eq. (4) [21] by considering its associated NLFPE in Eq. (1); the flux, representing the exchanges of entropy between the system and its neighborhood, is given by

$$\Phi = \frac{k}{D}\int_{-\infty}^{+\infty} dx\, A(x)J(x,t), \quad (8)$$

whereas the entropy-production contribution is given by

$$\Pi = \frac{k\eta}{D}\int_{-\infty}^{+\infty} dx\, \frac{\{J(x,t)\}^2}{\Psi[P]}. \quad (9)$$

Since k, η, D, and $\Psi[P(x,t)]$ were all defined previously as positive quantities, one obtains the desirable result $\Pi \geqslant 0$. Furthermore, when $A(x) = 0$, one has that $\Phi = 0$, representing a situation where there is no entropy flux between the system and its neighborhood; the stationary state, defined by $J(x,t) = 0$, yields $\Phi = \Pi = 0$.

The purpose of the present work is to investigate the quantities defined in Eqs. (8) and (9) for a system of superconducting vortices following an irreversible process, described by a NLFPE of the form of Eq. (1). In the next section, we define the model, its corresponding NLFPE, and the associated entropy $S_2(t)$, characteristic of nonextensive statistical mechanics. In Sec. III, we present data from molecular dynamics simulations, exhibiting the good agreement with analytical results, for both entropy production and entropy flux. Moreover, it is shown that the second law holds within the present framework, through an increase of $S_2(t)$ with time, up to its stationary-state value. Finally, in Sec. IV, we present our conclusions.

II. THE PHYSICAL SYSTEM AND ITS ASSOCIATED ENTROPY

Herein we will investigate the phenomenon of entropy production for a system of interacting vortices under overdamped motion. This system has been currently used in the literature to model flux lines in disordered type-II superconductors (see, e.g., Refs. [23–29]); the equation of motion of a flux line i under overdamped motion [i.e., with $(d\mathbf{v}_i/dt) = 0$], in a medium with an effective friction coefficient η, is given by

$$\eta\mathbf{v}_i = \mathbf{F}_i^{\rm pp} + \mathbf{F}_i^{\rm ext} \quad (i = 1,2,\cdots,N). \quad (10)$$

In the equation above, $\mathbf{v}_i$ represents the velocity, whereas the terms on the right-hand side depict the forces acting on flux line i. The particle-particle interactions $\mathbf{F}_i^{\rm pp}$ denote contributions from other vortices, whereas $\mathbf{F}_i^{\rm ext}$ represents an external force acting on vortex i. The vortex-vortex interactions are repulsive and radially symmetric, being expressed as [23,28,29]

$$\mathbf{F}_i^{\rm pp} = \frac{f_0}{2}\sum_{j\neq i} K_1(r_{ij}/\lambda)\,\hat{\mathbf{r}}_{ij}, \quad (11)$$

where $r_{ij} = |\mathbf{r}_i - \mathbf{r}_j|$ stands for the distance between vortices i and j, and $\hat{\mathbf{r}}_{ij} = (\mathbf{r}_i - \mathbf{r}_j)/r_{ij}$ is a vector defined along the axis joining them. Moreover, K_1 represents a modified Bessel function of the second kind of order one and f_0 is a positive constant. These interactions are defined in terms of a characteristic length scale λ, known as the London penetration length; other linear measures of this system are expressed in units of λ. The external forces $\mathbf{F}_i^{\rm ext}$ are associated to a confining type of potential, so that the system can reach a stationary state after a sufficiently long time. Herein this problem will be considered in a two-dimensional box of dimensions L_x and L_y, as carried in previous numerical simulations [30–32].

For an external force in the x direction, $\mathbf{F}^{\rm ext} = -A(x)\hat{\mathbf{x}}$, a coarse-graining procedure in Eq. (10) leads to the following NLFPE [29–31]:

$$\eta\frac{\partial P(x,t)}{\partial t} = -\frac{\partial[A(x)P(x,t)]}{\partial x} + 2D\frac{\partial}{\partial x}\left\{[\lambda P(x,t)]\frac{\partial P(x,t)}{\partial x}\right\}, \quad (12)$$

where $D = N\pi f_0\lambda^2/L_y$. It should be mentioned that this equation represents a particular case of the NLFPE usually considered in nonextensive statistical mechanics [33]. The time-dependent solution of this NLFPE is known for an initial condition $P(x,0) = \delta(x)$ and a harmonic external force $A(x) = -\alpha x$ ($\alpha > 0$),

$$P(x,t) = B(t)[1 - \beta(t)x^2]_+, \quad (13)$$

where $[y]_+ = y$, for $y > 0$, and zero otherwise, and the time-dependent coefficients $B(t)$ and $\beta(t)$ are related to each other in order to preserve the normalization of $P(x,t)$ for all times t [34,35]. One should notice that the distribution in Eq. (13) presents a compact support in the interval $[-\bar{x}(t),\bar{x}(t)]$, where $\bar{x}(t) = \beta^{-1/2}(t)$, being identified with a q-Gaussian distribution of nonextensive statistical mechanics with $q = 0$ [33,36].

Following Eqs. (3)–(5), in order to satisfy the H theorem, the entropy associated with the NLFPE of Eq. (12) should be given by [30–32]

$$S_2(t) = k\left\{1 - \lambda\int_{-\bar{x}(t)}^{\bar{x}(t)} dx\,[P(x,t)]^2\right\}. \quad (14)$$

Moreover, throughout the proof of the H theorem, one identifies the parameter θ, introduced in Eq. (3), with the

diffusion coefficient D of Eq. (12) by means of

$$k\theta \equiv D = \frac{N\pi f_0 \lambda^2}{L_y} = n\pi f_0 \lambda^2. \quad (15)$$

The quantity $k\theta$ presents dimension of energy and is directly related to the density $n = N/L_y$, as well as to the interactions among vortices, being always positive. According to recent advances in experimental techniques, the density of vortices became a controllable quantity [24–27], leading to the desirable possibility of varying θ. The analysis of Ref. [37] has shown that values of θ in type-II superconductors are much higher than typical room temperatures ($\theta \gg T$), so that the thermal noise can be neglected as a good approximation ($T/\theta \simeq 0$). In this case, certain thermodynamic properties, such as entropy and specific heat, become negligible within BG statistical mechanics; however, a curious situation concerning the third law of thermodynamics was verified in Ref. [30], where $S_{\rm BG} \to 0$, keeping the generalized entropic form $S_2 > 0$, as $T \to 0$.

Motivated by this, some stationary-state properties, related to the entropy S_2 and the internal energy in Eq. (3), were investigated for varying θ [37] by neglecting thermal noise. Moreover, by defining appropriately physical transformations, a Carnot cycle was constructed in Ref. [38], leading to an expression for its efficiency similar to the one of standard thermodynamics. These investigations have shown that θ plays a role in the present problem, analogous to the one of absolute temperature T in standard thermodynamics. Herein, we will investigate time-dependent properties, namely, the entropy production and flux associated with the entropic form $S_2(t)$, for different values of the parameter D of Eq. (15) by neglecting thermal noise.

In order to analyze the production of entropy $S_2(t)$, one needs to define a irreversible process associated with the above-defined physical system. For comparing analytical and numerical results, we will consider in the simulations an initial condition close to the one used for solving Eq. (12), which led to the solution in Eq. (13). The irreversible process investigated herein is shown in Fig. 1, and it consists of an expansion of the vortices across the rectangular box of linear sizes L_x and L_y. At time $t = 0$, the particles are packed around $x = 0$ (no excluded volume is considered), yielding strong repulsive interactions, in such a way that the particles move away very rapidly from the central region of the box. At larger times, the confining harmonic potential starts acting significantly so that the particles slow down, and for sufficiently long times, the repulsive and confining forces equilibrate, leading to an stationary state. During the expansion, one expects that $\Pi > 0$ and $\Phi \neq 0$, whereas $\Pi, \Phi \to 0$ as one approaches the stationary state. In the next section, we present data from molecular dynamics simulations, comparing them with results derived from the analytical solution of the associated NLFPE of Eq. (12).

III. ENTROPY PRODUCTION AND ENTROPY FLUX FOR VORTICES

By comparing Eqs. (1) and (12), one obtains, for the present case,

$$\Psi[P(x,t)] = P(x,t), \quad \Omega[P(x,t)] = 2\lambda P(x,t), \quad (16)$$

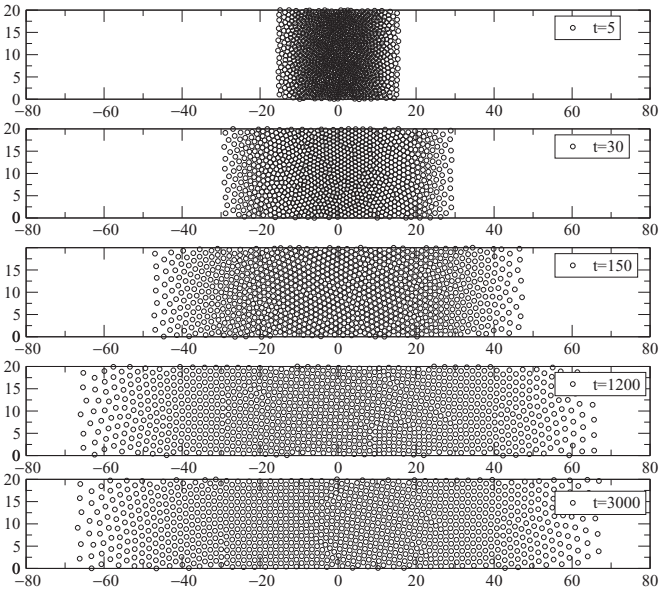

FIG. 1. The irreversible process investigated herein consists of an expansion of the vortices across the two-dimensional box; at time $t = 0$, the particles are packed around $x = 0$ (no excluded volume is considered) and the repulsive interactions dominate, in such a way that the particles move away very rapidly from the central region. At larger times, the confining harmonic potential starts acting significantly, so that the particles slow down, and for sufficiently long times the repulsive and confining forces equilibrate, leading to an stationary state. Several snapshots are presented, exhibiting the particle positions on typical times t, for a single sample of $N = 1000$ particles. In each snapshot, the horizontal and vertical axes (x/λ and y/λ, respectively) show the relevant part of a box of sizes $L_x = 280\lambda$ and $L_y = 20\lambda$. At $t = 5$, one has a state very close to the initial distribution, whereas the stationary state is essentially reached for $t = 1200$. The confining potential used was such that $\alpha = 10^{-3} f_0/\lambda$. The time is dimensionless, measured in terms of the molecular dynamics time step δt, as described in the text.

so that the NLFPE of Eq. (12) may be written in the form of Eq. (6), with the probability current

$$J(x,t) = \frac{1}{\eta}\left\{A(x)P(x,t) - 2\lambda D P(x,t)\left[\frac{\partial P(x,t)}{\partial x}\right]\right\}. \quad (17)$$

It is important to notice that the solution in Eq. (13) presents a compact support, being nonzero inside the interval $[-\bar{x}(t),\bar{x}(t)]$, and zero otherwise. Moreover, the time-dependent parameters $\bar{x}(t)$, $B(t)$, and $\beta(t)$ are not all independent. Indeed, imposing $P[\bar{x}(t),t] = 0$ yields $\bar{x}(t) = \beta^{-1/2}(t)$, and in order to guarantee normalization for all times, the parameters $B(t)$ and $\beta(t)$ should be related by [34,35]

$$\frac{\beta(t)}{\beta(t_0)} = \left[\frac{B(t)}{B(t_0)}\right]^2, \quad (18)$$

where t_0 represents a reference time. For the distribution in Eq. (13), one obtains [31]

$$B(t) = B(t_0)(K_2)^{1/3}[1 + (K_2 - 1)\exp(-3\alpha t)]^{-1/3}, \quad (19)$$

$$\beta(t) = \beta(t_0)(K_2)^{2/3}[1 + (K_2 - 1)\exp(-3\alpha t)]^{-2/3}, \quad (20)$$

$$K_2 = \frac{\alpha}{4D\lambda\beta(t_0)B(t_0)}. \quad (21)$$

Hence, for given values of α, D, $B(t_0)$, and $\beta(t_0)$, one may use Eqs. (19)–(21) to obtain the time-dependent parameters $B(t)$, $\beta(t)$, and, consequently, $\bar{x}(t)$.

Considering the results above, the boundary conditions of Eq. (2) yield

$$P(x,t)|_{x=\pm\bar{x}} = 0, \quad \left.\frac{\partial P(x,t)}{\partial x}\right|_{x=\pm\bar{x}} = \mp 2B(t)\beta(t)\bar{x}(t),$$

$$A(x)P(x,t)|_{x=\pm\bar{x}} = 0, \quad J(x,t)|_{x=\pm\bar{x}} = 0 \ \ (\forall t). \quad (22)$$

Therefore, one can calculate all of the relevant quantities above analytically, which by using that $\bar{x}(t) = \beta^{-1/2}(t)$, their time dependence appears through the parameters $B(t)$ and $\beta(t)$ of Eqs. (19)–(21). One gets

$$\frac{S_2(t)}{k} = 1 - \frac{16}{15}\lambda B^2(t)\beta^{-1/2}(t), \quad (23)$$

$$\eta J(x,t) = B(t)[x - \beta(t)x^3][4\lambda D B(t)\beta(t) - \alpha], \quad (24)$$

$$\Phi(t) = \frac{4}{15}\frac{k\alpha B(t)}{\eta D\beta^{3/2}(t)}\left[\alpha - 4\lambda D B(t)\beta(t)\right], \quad (25)$$

$$\Pi(t) = \frac{4}{15}\frac{k B(t)}{\eta D\beta^{3/2}(t)}\left[\alpha - 4\lambda D B(t)\beta(t)\right]^2, \quad (26)$$

leading to

$$\frac{dS_2(t)}{dt} = \Pi(t) - \Phi(t) = \frac{16}{15}\frac{k\lambda B^2(t)}{\eta\sqrt{\beta(t)}}\left[4\lambda D B(t)\beta(t) - \alpha\right]. \quad (27)$$

From Eqs. (19)–(21), one verifies that $B(t),\beta(t) \geqslant 0$ with $4\lambda D B(t)\beta(t) \geqslant \alpha$, leading to $\Phi(t) \leqslant 0$, $\Pi(t) \geqslant 0$, and $[dS_2(t)/dt] \geqslant 0$ in the equations above. Hence, the stationary state is attained in the limit $4\lambda D B(t)\beta(t) \to \alpha$, where the quantities of Eqs. (24)–(27) all vanish. In these quantities, one sees clearly a competition between the time-dependent term multiplied by the diffusion constant D and the constant α associated with the harmonic confining potential. Along the whole time evolution, the former contribution is stronger, approaching a constant value that is precisely α at the stationary state. Moreover, considering this limit, in addition to the choice for the initial values $[B^2(t_0)/\beta(t_0)] = (3/4)^2$, one obtains the stationary-state entropy [37–39]

$$\frac{S_2^{(\mathrm{stat})}}{k} = 1 - \frac{3^{2/3}}{5}\left(\frac{\alpha\lambda^2}{k\theta}\right)^{1/3}. \quad (28)$$

For numerical purposes, we replace the initial condition, $P(x,0) = \delta(x)$, by a narrow uniform distribution, considering all particles spread throughout a small region around $x = 0$ at $t = 0$; this avoids numerical difficulties caused by interacting vortices separated by very small distances. The particular choice of the parameter α is directly associated with the time taken by the system to reach its stationary state; as will be seen next, the qualitative physical behavior of the quantities above is unaltered by this choice. However, the choice of D is related to the linear density of particles, $n = N/L_y$, as defined in Eq. (15). In the numerical simulations that follow, we have used two different choices for the confining constant α, namely, $\alpha = 10^{-3} f_0/\lambda$ (associated with a larger time for reaching the stationary state) and $\alpha = 10^{-2} f_0/\lambda$ (associated with a shorter time for reaching the stationary state). Using Eq. (15), the quantity $2D\lambda$ that appears in the NLFPE of Eq. (12), as well as in Eq. (17), is given by $2D\lambda = n(2\pi f_0\lambda^3)$, which, in principle, may differ from the numerical estimate. In fact, in order to fit the theoretical results with the numerical ones, we have used $2D\lambda = n[(5.87 \pm 0.02) f_0\lambda^3]$, where the error bars come from the best least-squares fits of the theoretical curves. Such a disagreement between analytical and numerical estimates (leading to a relative discrepancy around 7%) is a direct consequence of the coarse-graining approximation carried for obtaining the NLFPE of Eq. (12) [30,31]. We simulated systems with three different values for the total number of particles, namely, $N = 4000, 2000$, and 1000. The particles were confined in a two-dimensional box of sizes $L_x = 280\lambda$ and $L_y = 20\lambda$, with periodic boundary conditions in the y direction. These choices lead to three distinct linear density of vortices, $n = (200/\lambda), (100/\lambda)$, and $(50/\lambda)$, respectively, and, consequently, three different values of the parameter D.

In Fig. 2, we present the time behavior of the parameters $B(t)$ [Fig. 2(a)] and $\beta(t)$ [Fig. 2(b)] of the distribution in Eq. (13) in a linear-log representation. The symbols are numerical data, whereas the full lines correspond to the analytical results. In each case, two choices for the confining constant were employed, namely, $\alpha = 10^{-3} f_0/\lambda$ and $\alpha = 10^{-2} f_0/\lambda$ (in the respective insets). The number of particles considered was $N = 4000$, leading to a linear density of particles $n = (200/\lambda)$. One sees that the higher value of α yields a much faster approach to the stationary state, although the qualitative time behavior of the parameters does not change.

The probability current $J(x,t)$ of Eq. (17) [or, equivalently, Eq. (24)] is represented versus the position in Fig. 3. Usually, this quantity presents dimensions $[\mathrm{time}]^{-1}$, and since herein time is dimensionless (measured in terms of the molecular dynamics time step δt), $J(x,t)$ is dimensionless. In Fig. 3(a), we represent $J(x,t)$ versus x/λ for typical times of the evolution. One sees that the probability current is zero for $x = 0$, since $A(x)|_{x=0} = 0$, as well as $[\partial P(x,t)/\partial x]|_{x=0} = 0$; in addition to this, the boundary conditions of Eq. (22) also give $J(x,t)|_{x=\pm\bar{x}} = 0$ $(\forall t)$. Furthermore, the symmetry $J(-x,t) = -J(x,t)$ $(\forall t)$ is seen clearly in Fig. 3(a). The absolute value of the probability current, $|J(x,t)|$, presents more significant values for shorter times when the probability distribution is changing more rapidly, becoming smaller as time increases, in such a way that $|J(x,t)| \to 0$ for sufficiently large times. Interestingly, there is always a value of $|x/\lambda|$ for which $|J(x,t)|$ becomes maximum. The dimensionless quantities $[J(x,t)/J^*(t)]$ versus $[x/\bar{x}(t)]$ are presented in Fig. 3(b), where $J^*(t)$ is calculated as the maximum value of $J(x,t)$, for each time t. For the variables used in Fig. 3(b), data from distinct times collapse into a single universal curve, such that one has a maximum of $|J(x,t)/J^*(t)|$ for $|x/\bar{x}(t)| \approx 0.6$. Therefore, one has a situation where $[\partial J(x,t)/\partial x]_{|x/\bar{x}(t)|\approx 0.6} = 0$ $(\forall t)$, for which the distribution of Eq. (13) becomes $P(x,t) \approx 0.64B(t)$. It should be mentioned that this represents a physical situation distinct from the stationary state, since the probability distribution presents a

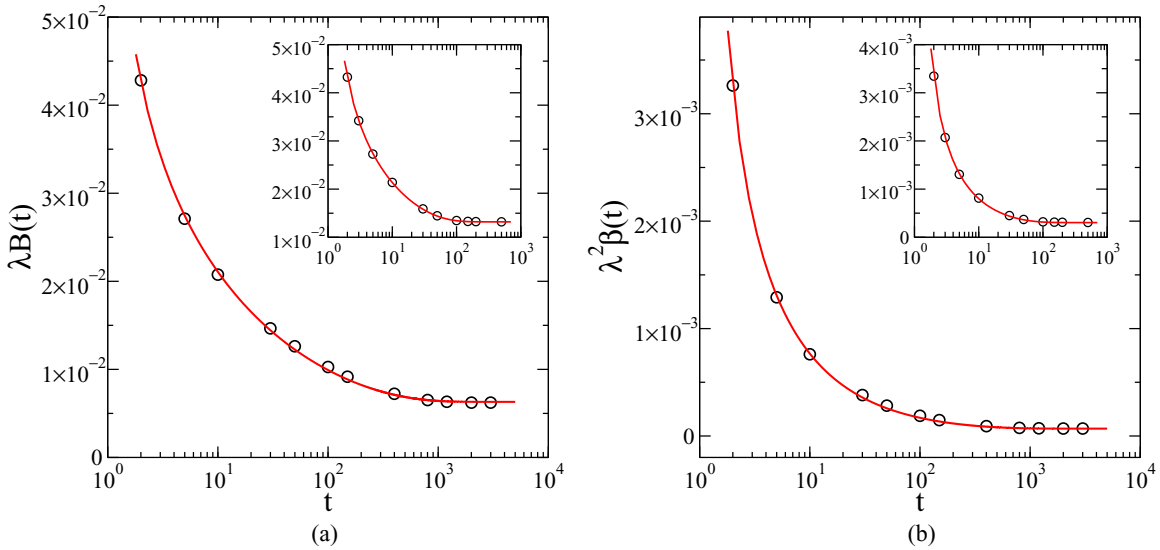

FIG. 2. (Color online) The dimensionless time-dependent parameters (a) $\lambda B(t)$ and (b) $\lambda^2\beta(t)$ of the distribution in Eq. (13) are represented vs time. The symbols are numerical data, whereas the full lines correspond to the analytical results. In each case, two choices for the confining constant were employed, namely, $\alpha = 10^{-3} f_0/\lambda$ ($\alpha = 10^{-2} f_0/\lambda$ in the respective insets). The linear density of particles considered was $n = (200/\lambda)$ [i.e., $D = 200\pi f_0\lambda$]. The time is dimensionless, measured in terms of the molecular dynamics time step δt.

time dependence. The results of Figs. 2 and 3 give evidence of the good agreement between data from the numerical simulations and the analytical results, derived from the NLFPE of Eq. (12). They strongly support the close relation between the dynamics of the system of vortices studied herein and such a NLFPE; this will be reinforced throughout the following results.

In Fig. 4, we present the entropy production [Fig. 4(a)] and entropy flux [Fig. 4(b)] as a function of time. Three different choices of the parameter D were considered by choosing conveniently the total number of vortices, $N = 4000$, $N = 2000$, and $N = 1000$, corresponding to $D = 200\pi f_0\lambda$, $D = 100\pi f_0\lambda$, and $D = 50\pi f_0\lambda$, respectively. From Fig. 4(a), one notices that $\Pi(t) \geqslant 0(\forall t)$, as expected, whereas the stationary state is reached (within our numerical accuracy) for $[\Pi(t)/k] < 10^{-6}$. Moreover, for two given values $D_1 > D_2$, one sees that the quantities of Fig. 4 are such that $\Phi_1(t) \geqslant \Phi_2(t)$, whereas $\Pi_1(t) \leqslant \Pi_2(t)$ $(\forall t)$. In the present

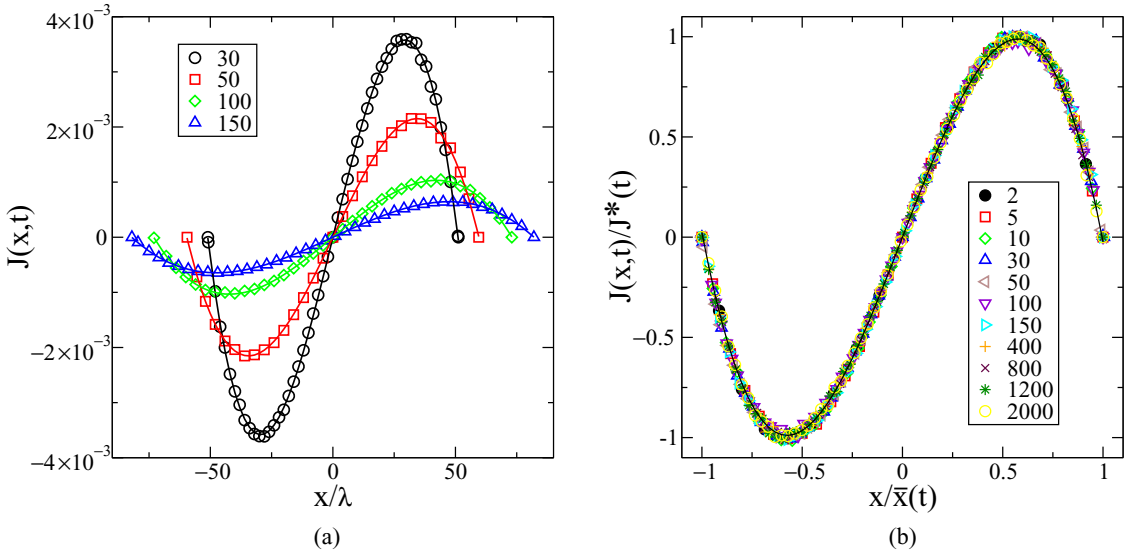

FIG. 3. (Color online) (a) The dimensionless probability current $J(x,t)$ [cf. Eq. (17) or, equivalently, Eq. (24)] is exhibited vs the position x (in units of λ) for typical times of the evolution (shown as different symbols). The symbols are numerical data, whereas the full lines correspond to the analytical results. (b) The same quantity is presented in a conveniently scaled representation, where data from different times (shown as distinct symbols) collapse into a single universal curve; the full line stands for the analytical result. Both ordinate and abscissa are dimensionless quantities, and in the former, $J^*(t)$ represents the maximum value of $J(x,t)$ at time t, whereas in the latter, $\bar{x}(t)$ depicts the compact support of the distribution, as described in the text. The results presented correspond to a confining constant $\alpha = 10^{-3} f_0/\lambda$ and to a linear density of particles $n = (200/\lambda)$, i.e., $D = 200\pi f_0\lambda$.

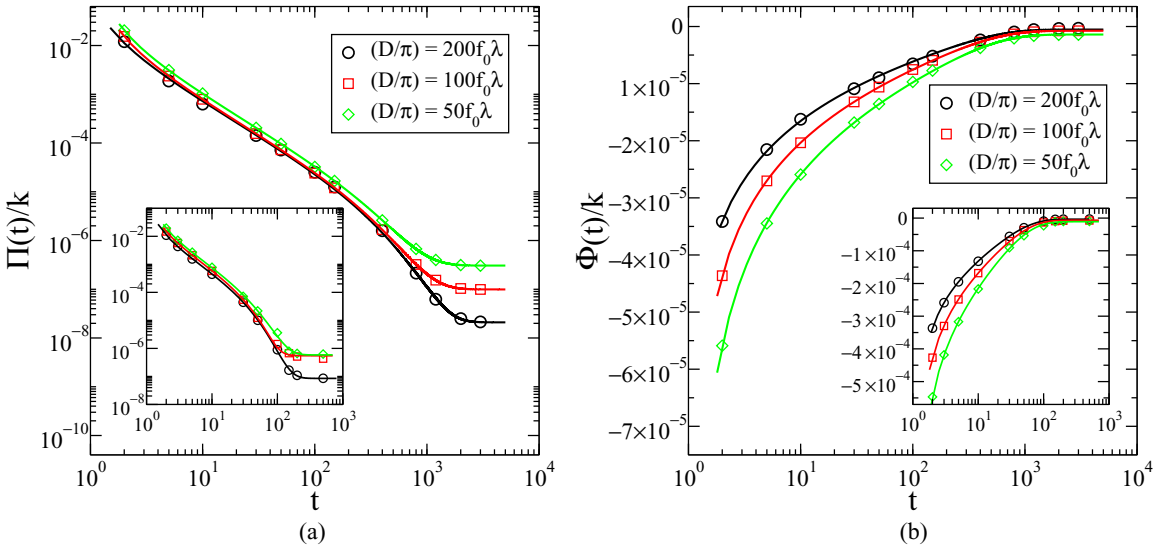

FIG. 4. (Color online) The entropy production $\Pi(t)$ and entropy flux $\Phi(t)$, defined in Eqs. (7)–(9) [see also Eqs. (25) and (26)], are presented vs time. The symbols are numerical data, whereas the full lines correspond to the analytical results. In each case, two choices for the confining constant were employed, namely, $\alpha = 10^{-3} f_0/\lambda$ ($\alpha = 10^{-2} f_0/\lambda$ in the respective insets). Three different values for the total number of vortices were chosen conveniently, leading to three distinct values of the parameter D [cf. Eq. (15)], namely, $D = 200\pi f_0\lambda$, $D = 100\pi f_0\lambda$, and $D = 50\pi f_0\lambda$. The time is dimensionless, measured in terms of the molecular dynamics time step δt.

irreversible process, one has that $\Phi(t) \leqslant 0$, as discussed above and illustrated in Fig. 4(b); consequently, in this case, Eq. (7) may be rewritten as

$$\frac{dS_2(t)}{dt} = \Pi(t) + |\Phi(t)|, \tag{29}$$

from which one concludes that the external force $A(x)$ enlarges the time rate of the entropy, resulting from a flux of entropy towards the system. As mentioned before, the confining constant does not qualitatively affect the quantities presented in Fig. 4; one sees that the higher choice, $\alpha = 10^{-2} f_0/\lambda$ (see insets), decreases the time for reaching the stationary state (typically by a factor of 10), but keeps a similar qualitative time behavior for both $\Pi(t)$ and $\Phi(t)$.

The entropy time rate and entropy $S_2(t)$ are represented versus time in Figs. 5(a) and 5(b), respectively. Three different

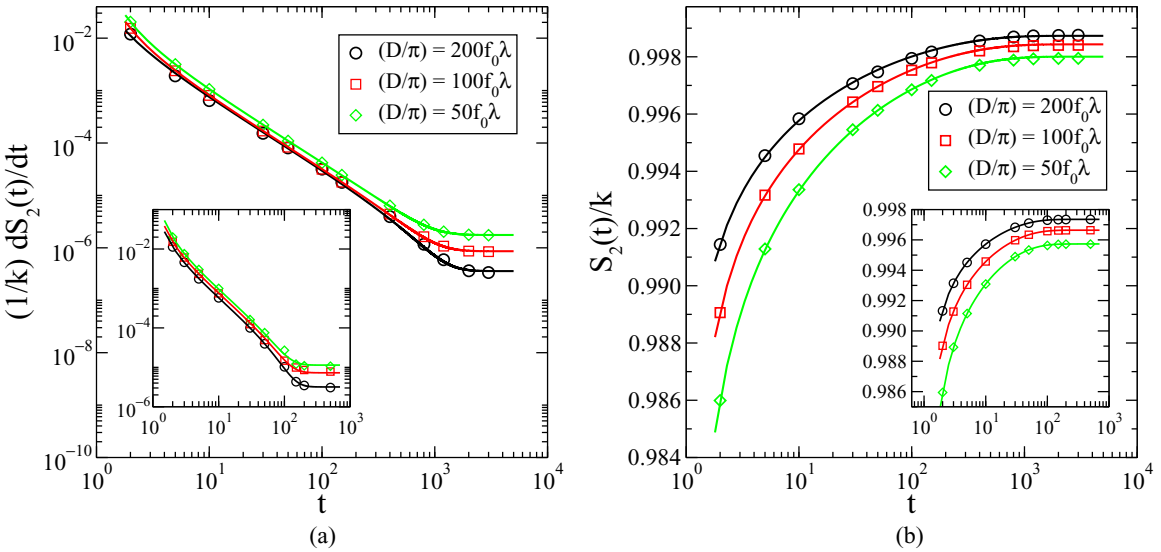

FIG. 5. (Color online) The time rate of the entropy, as well as the entropy of Eq. (14) [see also Eqs. (23) and (27)], are represented vs time. The symbols are numerical data, whereas the full lines correspond to the analytical results. In each case, two choices for the confining constant were employed, namely, $\alpha = 10^{-3} f_0/\lambda$ ($\alpha = 10^{-2} f_0/\lambda$ in the respective insets). Three different values for the total number of vortices were chosen conveniently, leading to $D = 200\pi f_0\lambda$, $D = 100\pi f_0\lambda$, and $D = 50\pi f_0\lambda$. At the stationary state, these choices correspond to three distinct values of the effective temperature θ [cf. Eq. (15)]. The increase of the total entropy with time, presented in (b), shows that the second law of thermodynamics applies also for the entropic form of Eq. (14), within the present irreversible process. The time is dimensionless, measured in terms of the molecular dynamics time step δt.

values for the total number of vortices were chosen conveniently and, at the stationary state, these choices correspond to three distinct values of the effective temperature θ [cf. Eq. (15)]. Comparing Fig. 5(a) with Figs. 4(a) and 4(b), one notices that $dS_2(t)/dt$ presents essentially the same qualitative behavior exhibited by $\Pi(t)$.

In standard thermodynamics, higher temperatures are associated with an increase of disorder, leading to higher values of entropy; a similar situation is found in the present problem, as shown in Fig. 5(b), where at the stationary state one defines an effective temperature according to Eq. (15). In this figure, one observes an approach to the stationary-state entropy of Eq. (28), which was obtained from the time-dependent behavior of Eq. (23) by considering the stationary-state limit and a particular choice for the relation involving the initial values $B(t_0)$ and $\beta(t_0)$. In order to provide a good visualization of the time-dependent behavior, we had to choose parameters in the present process such that in the entropy of Eq. (28), $\alpha\lambda^2 \ll k\theta$, leading to $(S_2^{(\mathrm{stat})}/k) \approx 1$; the time behavior of $S_2(t)$ for a higher choice of α is shown in the respective inset.

The most important conclusion that emerges from Fig. 5 concerns the second law of thermodynamics, which appears as $(dS_2(t)/dt) \geqslant 0$ [Fig. 5(a)] or, more clearly, with the increase of $S_2(t)$ with time [Fig. 5(b)]. Hence, the second law of thermodynamics is illustrated herein for an irreversible process in a physical system described by the entropic form of Eq. (14), in which thermal effects were neglected. Moreover, as expected physically, for a fixed time t one sees that systems with higher values of D and, consequently, higher values of the effective temperature θ at the stationary state present larger values of entropy.

IV. CONCLUSIONS

General proofs of the H theorem have been achieved recently, in order to relate nonlinear Fokker-Planck equations with generalized entropic forms. Within this framework, a model of superconducting vortices following an overdamped motion has been identified to a nonlinear Fokker-Planck equation and, consequently, to an entropic form $S_2(t)$, characteristic of nonextensive statistical mechanics [30,31]. In this work, we have considered an irreversible process for this system and, based on its associated nonlinear Fokker-Planck, we have studied the phenomenon of entropy production. The system is studied in a regime where thermal effects can be neglected, and so contributions from the Boltzmann-Gibbs entropy are disregarded. Both contributions of the entropy time rate $[dS_2(t)/dt]$ were analyzed, namely, the entropy production and entropy flux from the system to its surroundings. Moreover, we have shown that the second law holds also within the present framework, through an increase of $S_2(t)$ with time up to its stationary-state value, in spite of the absence of thermal noise. All analytical results have been compared with numerical data from molecular dynamics simulations carried for this process, and a good agreement between both has been shown.

The present results yield further evidence that interacting vortices under overdamped motion, which define a model currently used for describing type-II superconductors, is related to nonextensive statistical mechanics. In addition to the consistent thermodynamical framework developed for its stationary state in the absence of thermal noise, presented in Refs. [37–39], we have shown herein that important time-dependent behavior associated with $S_2(t)$, such as entropy production, entropy flux, as well as a manifestation of the second law, also hold for this system.

ACKNOWLEDGMENTS

We thank C. Tsallis and E. M. F. Curado for fruitful conversations. The partial financial support from CNPq and FAPERJ (Brazilian agencies) is acknowledged.

[1] S. R. de Groot and P. Mazur, *Non-Equilibrium Thermodynamics* (Dover, New York, 1984).
[2] L. E. Reichl, *A Modern Course in Statistical Physics*, 2nd ed. (Wiley, New York, 1998).
[3] T. D. Frank, *Nonlinear Fokker-Planck Equations: Fundamentals and Applications* (Springer, Berlin, 2005).
[4] M. Shiino, J. Math. Phys. **42**, 2540 (2001).
[5] T. D. Frank and A. Daffertshofer, Physica A **295**, 455 (2001).
[6] P. H. Chavanis, Phys. Rev. E **68**, 036108 (2003).
[7] V. Schwämmle, F. D. Nobre, and E. M. F. Curado, Phys. Rev. E **76**, 041123 (2007).
[8] V. Schwämmle, E. M. F. Curado, and F. D. Nobre, Eur. Phys. J. B **58**, 159 (2007).
[9] V. Schwämmle, E. M. F. Curado, and F. D. Nobre, Eur. Phys. J. B **70**, 107 (2009).
[10] M. S. Ribeiro, F. D. Nobre, and E. M. F. Curado, Entropy **13**, 1928 (2011).
[11] J. P. Bouchaud and A. Georges, Phys. Rep. **195**, 127 (1990).
[12] I. Prigogine, *Introduction of the Thermodynamics of Irreversible Processes* (Wiley, New York, 1967).
[13] P. Glansdorff and I. Prigogine, *Thermodynamic Theory of Structure, Stability and Fluctuations* (Wiley, New York, 1971).
[14] G. Nicolis and I. Prigogine, *Self-Organization in Nonequilibrium Systems* (Wiley, New York, 1977).
[15] J. Schnakenberg, Rev. Mod. Phys. **48**, 571 (1976).
[16] T. Tomé, Braz. J. Phys. **36**, 1285 (2006).
[17] T. Tomé and M. J. de Oliveira, Phys. Rev. E **82**, 021120 (2010).
[18] A. Compte and D. Jou, J. Phys. A **29**, 4321 (1996).
[19] K. H. Hoffmann, C. Essex, and C. Schulzky, J. Non-Equilib. Thermodyn. **23**, 166 (1998).
[20] C. Essex, C. Schulzky, A. Franz, and K. H. Hoffmann, Physica A **284**, 299 (2000).
[21] G. A. Casas, F. D. Nobre, and E. M. F. Curado, Phys. Rev. E **86**, 061136 (2012).
[22] G. A. Casas, F. D. Nobre, and E. M. F. Curado, Phys. Rev. E **89**, 012114 (2014).
[23] C. P. Poole, Jr., H. A. Farach, and R. J. Creswick, *Superconductivity* (Academic, London, 1995).
[24] C.-S. Lee, B. Jankó, I. Derényi, and A.-L. Barabási, Nature (London) **400**, 337 (1999).
[25] I. Derényi, Appl. Phys. A **75**, 217 (2002).

[26] J. E. Villegas, S. Savel'ev, F. Nori, E. M. Gonzalez, J. V. Anguita, R. García, and J. L. Vicent, Science **302**, 1188 (2003).
[27] B. Y. Zhu, F. Marchesoni, and F. Nori, Phys. Rev. Lett. **92**, 180602 (2004).
[28] H. J. Jensen, A. Brass, and A. J. Berlinsky, Phys. Rev. Lett. **60**, 1676 (1988); O. Pla and F. Nori, *ibid.* **67**, 919 (1991); R. A. Richardson, O. Pla, and F. Nori, *ibid.* **72**, 1268 (1994).
[29] S. Zapperi, A. A. Moreira, and J. S. Andrade, Phys. Rev. Lett. **86**, 3622 (2001).
[30] J. S. Andrade, Jr., G. F. T. da Silva, A. A. Moreira, F. D. Nobre, and E. M. F. Curado, Phys. Rev. Lett. **105**, 260601 (2010).
[31] M. S. Ribeiro, F. D. Nobre, and E. M. F. Curado, Phys. Rev. E **85**, 021146 (2012).
[32] M. S. Ribeiro, F. D. Nobre, and E. M. F. Curado, Eur. Phys. J. B **85**, 309 (2012).
[33] C. Tsallis, *Introduction to Nonextensive Statistical Mechanics* (Springer, New York, 2009).
[34] A. R. Plastino and A. Plastino, Physica A **222**, 347 (1995).
[35] C. Tsallis and D. J. Bukman, Phys. Rev. E **54**, R2197 (1996).
[36] C. Tsallis, Entropy **13**, 1765 (2011).
[37] F. D. Nobre, A. M. C. Souza, and E. M. F. Curado, Phys. Rev. E **86**, 061113 (2012).
[38] E. M. F. Curado, A. M. C. Souza, F. D. Nobre, and R. F. S. Andrade, Phys. Rev. E **89**, 022117 (2014).
[39] R. F. S. Andrade, A. M. C. Souza, E. M. F. Curado, and F. D. Nobre, Europhys. Lett. **108**, 20001 (2014).